DISCREPANCY BETWEEN FUNDUS AUTOFLUORESCENCE ABNORMALITY AND VISUAL FIELD LOSS IN BIETTI CRYSTALLINE DYSTROPHY

DAIKI SAKAI, MD,*†‡ TADAO MAEDA, MD, PhD,* AKIKO MAEDA, MD, PhD,*†
MIDORI YAMAMOTO, BA,* SATOSHI YOKOTA, MD, PhD,*† YASUHIKO HIRAMI, MD, PhD,*‡
MAKOTO NAKAMURA, MD, PhD,‡ MASAYO TAKAHASHI, MD, PhD,* MICHIKO MANDAI, MD, PhD,*†
YASUO KURIMOTO, MD, PhD*†

Purpose: The aim of this study was to explore the potential benefits of retinal pigment epithelium replacement therapy in patients with Bietti crystalline dystrophy (BCD) by assessing the disease pathology with the distinctive relationship between fundus autofluorescence (FAF) abnormality and visual field defect.

Methods: Sixteen eyes from 16 patients with BCD and 16 eyes from 16 patients with RHO-associated retinitis pigmentosa were included. Fundus autofluorescence, optical coherence tomography, and Goldmann perimetry results were retrospectively reviewed and assessed using image analyses.

Results: In patients with BCD, the FAF abnormality area was not correlated with the overall visual field defect area and median overall visual field defect area (57.5%) was smaller than FAF abnormality area (98.5%). By contrast, the ellipsoid zone width was significantly correlated with the central visual field area (r = 0.806, $P < 0.001$). In patients with RHO-associated retinitis pigmentosa, the FAF abnormality area and ellipsoid zone width were significantly correlated with the overall visual field defect area (r = 0.833, $P < 0.001$) and central visual field area (r = 0.887, $P < 0.001$), respectively.

Conclusion: The FAF abnormality shown in patients with BCD involves retinal pigment epithelium degeneration without complete loss of photoreceptors or visual function. These results suggest that patients with BCD are good candidates for retinal pigment epithelium replacement therapy for preservation of residual visual function.

RETINA 44:1394–1402, 2024

Inherited retinal degenerative diseases (IRDs) are a clinically and genetically heterogeneous group of disorders that are a major cause of blindness in developed countries.[1] The diagnosis of IRDs once implied incurable disease progression, regardless of the phenotype or genotype. However, recent advancements in research have led to the emergence of new therapeutic options, encouraging us to assess the disease heterogeneity and categorize different conditions in patients with IRDs to assign appropriate therapy.

Pluripotent stem cell–derived retinal pigment epithelium (RPE) transplantation is expected to be a potential therapy for intractable retinal diseases.[2] We have confirmed the safety and efficacy of induced pluripotent stem cell–derived RPE transplantation in clinical research studies of age-related macular degeneration.[3,4] Furthermore, the current ongoing clinical research expands the application of this therapy to include other retinal diseases with RPE dysfunction or degeneration (registered in the Japanese Registry of Clinical Trials, jRCTa050210178).

One of the candidate diseases for the RPE replacement therapy is Bietti crystalline dystrophy (BCD), a rare form of IRDs characterized by unique fundus appearance with a myriad of yellowish glittering crystalline deposits, followed by progressive RPE, choroid, and subsequent outer retinal degeneration. The causative gene of BCD is *CYP4V2*, which encodes a member of the cytochrome P450 family of enzymes that play a role in lipid metabolism.[5] It has been

postulated that RPE dysfunction is a primary pathology in BCD,[6,7] although the mechanism of retinal degeneration is not fully understood. The disease progression of BCD is distinct from that of retinitis pigmentosa (RP), which is the most common form of IRDs. In BCD, chorioretinal atrophy expands centrifugally from the posterior pole toward the periphery,[8] whereas in RP, concentric centripetal progression is typical.

Fundus autofluorescence (FAF) is a noninvasive retinal imaging technique that has become an established methodology for observing disease progression in both BCD[9,10] and RP.[11] The original source of FAF is lipofuscin in the RPE,[12] and abnormal autofluorescence is thought to represent unhealthiness or atrophy of the RPE. The RPE is an indispensable partner of the neural retina.[13] Photoreceptors over unhealthy RPE are destined to degenerate, or conversely, photoreceptor degeneration causes RPE atrophy. Thus, in the region of FAF abnormality, the status of photoreceptors is supposed to be in the process of degeneration. A good consistency between abnormal FAF areas and visual field defects has been demonstrated in RP,[11,14] which

From the *Department of Ophthalmology, Kobe City Eye Hospital, Kobe, Japan; †Department of Ophthalmology, Kobe City Medical Center General Hospital, Kobe, Japan; and ‡Division of Ophthalmology, Department of Surgery, Kobe University Graduate School of Medicine, Kobe, Japan.

implies that FAF abnormality in patients with RP is generally accompanied by photoreceptors and visual function defects. By contrast, patients with BCD whose FAF exhibited extensive RPE atrophy could have almost normal electroretinogram responses.[15] This suggests that BCD, having the regions of functional retina but with RPE degeneration, can be a good indication for the RPE replacement therapy. To date, there is no comprehensive report that investigates the relationship between the degree of RPE degeneration and that of photoreceptor damage or visual function defects in patients with BCD. This study aimed to explore the potential benefits of the RPE transplantation therapy for patients with BCD by assessing the characteristic pathology through the relationship between FAF abnormality and VF defects.

Methods

Study Design

This study adhered to the principles of the Declaration of Helsinki and was approved by the Medical Ethics Committee of Kobe City Medical Center General Hospital (Kobe, Japan). All patients provided written informed consent to participate in this study before undergoing genetic testing.

Patients

We reviewed the medical records of patients with genetically confirmed *CYP4V2*-associated BCD who visited the IRDs clinic at Kobe City Eye Hospital between December 2017 and September 2022. In addition, patients with *RHO*-associated RP (RHO-RP)[16] who visited the IRD clinic during the same time period were assessed for comparison.

We included only the patients who underwent Goldmann perimetry and wide-field FAF (permitted time interval between these two examinations was within 4 months). Earlier results were used if the patients had multiple visits. The exclusion criteria were poor image quality of wide-field FAF, a history of confounding ocular pathologies that could affect VF, and previous invasive treatments. We excluded two eyes in two patients with BCD who had a history of acute primary angle closure and choroidal neovascularization. Moreover, we excluded six eyes in four patients with *RHO*-RP (bilateral glaucoma, four eyes; optic neuritis, one eye; and ocular trauma, one eye). If both eyes in one patient were available, the eye with better best-corrected visual acuity was selected; when the patient had the same best-corrected visual acuity in both eyes, one eye was randomly selected.

Wide-field Fundus Autofluorescence

Wide-field FAF images were obtained using Optos 200Tx (Optos PLC; Dunfermline, Scotland, United Kingdom) after pupil dilation with topical phenylephrine. Two researchers (D.S. and M.Y.) identified hypoautofluorescent areas on FAF through discussion. Consequently, the following image assessment was performed using ImageJ software (http://imagej.nih.gov/ij/, provided in the public domain by the National Institutes of Health, Bethesda, MD).[11,14] An elliptical area of $3,000 \times 2,100$ pixels (theoretically equivalent to $154 \times 108°$) was trimmed from the original image ($3,900 \times 3,072$ pixels) to compensate for the image distortion that was remarkable in the peripheral retina. Hypoautofluorescent areas were manually traced and measured by one observer (D.S.). This measurement was performed twice in each patient, and the average value was used for analysis. Fundus autofluorescence abnormality area (%) was defined as the percentage of the cumulative area of hypoautofluorescent FAF to the entire trimmed area (Figure 1).
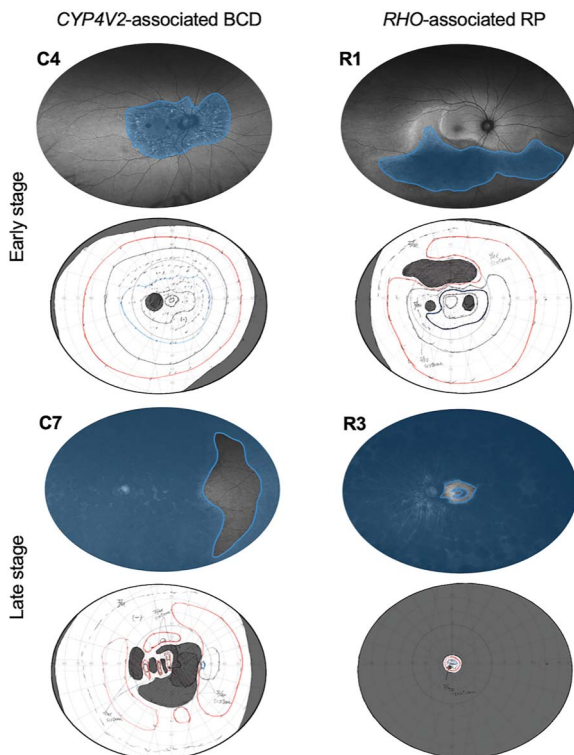

Fig. 1. Representative images of FAF and Goldmann perimetry for image assessment. The left-hand vertical row presents the images obtained from patients with BCD, and the right-hand row presents those obtained from patients with *RHO*-RP. The regions shaded in blue-gray represent the FAF abnormality area and the overall VF defect area.

Visual Field

Kinetic VF testing was performed using Goldmann perimetry (Haag Streit, Bern, Germany). The results were scanned and registered using ImageJ software. Visual field defect areas were determined as follows: First, an area of 60° superiorly, 90° temporally, 70° inferiorly, and 70° nasally, referring to normal VF extension, was trimmed from the original chart.[14] Then, the accumulation of defect areas of the V4e isopter and scotoma areas of the I4e isopter was measured, and its percentage for the trimmed area was defined as the overall VF defect (VFD) area (%) (Figure 1). In addition, the remaining VF area within 30° in diameter was measured as the area inside the V4e isopter excluding the I4e scotoma area, and its percentage for the total area of a circle with a diameter of 30° was defined as the central VF area (%) (Figure 2). These measurements were repeated twice by one observer (D.S.), and the average value of the two measurements was used.

Optical Coherence Tomography

We reviewed the spectral domain optical coherence tomography (OCT) images obtained at the closest visit to the VF testing visit. Cross-sectional OCT images along the horizontal/vertical meridian through the fovea were obtained using Spectralis (Heidelberg Engineering), covering a macular area of approximately $30 \times 30°$. The ellipsoid zone (EZ) width was measured using the "caliper" function of the Heidelberg instrument. The ellipsoid zone width was defined as the distance between the superior and inferior borders of the visible EZ line or their accumulation in cases where the EZ lines were intermittent (Figure 2). If the length of the EZ line exceeded the size of the OCT image, the borders of the EZ were considered to be those of the OCT image.[17] The EZ width measurements were performed twice by one observer (D.S.), and the average values were recorded. The horizontal and vertical EZ widths were acquired from the horizontal and vertical OCT images, respectively. Subsequently, the average of these horizontal and vertical EZ widths was defined as the representative EZ width for each patient. Three patients with macular pathologies (one with BCD who had submacular exudates and two with *RHO*-RP who had epiretinal membrane) that affect the OCT measurement were excluded from this analysis.

Visual Acuity

Best-corrected visual acuity was determined using Landolt C-charts and converted to logarithm of the
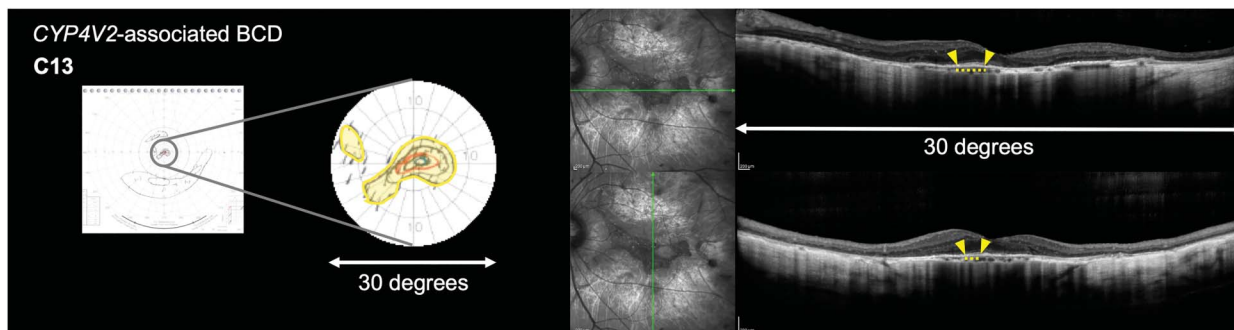
Fig. 2. Representative images of Goldmann perimetry and OCT in a patient with BCD. The central VF area is measured as the area inside the V4e isopter (excluding I4e scotoma area) within central 30° in diameter on Goldmann perimetry (shaded in yellow). The EZ width is measured in cross-sectional OCT images (yellow arrow heads and dashed lines).

minimum angle of resolution equivalent for statistical comparisons. Extremely low visual acuity was converted to values of 2.0 for counting fingers and 2.3 for hand motion.[18] Patients whose visual acuity was light perception or no light perception were excluded from the visual acuity assessment.[19]

Genetic Diagnosis

Between 2008 and 2022, the study participants underwent at least one genetic screening for diagnosis. Genetic testing was performed by stepwise Sanger sequencing using one or two panels of 15 and 27 genes during 2008 to 2015[20] or next-generation sequencing using panels of 39 or 50 genes during 2015 to 2019[21] or 2019 and later.[22,23] Genetic testing was performed at the Institute of Biomedical Research and Innovation Hospital between November 2008 and September 2017 and at Kobe City Eye Hospital between December 2017 and September 2022 (the Institute of Biomedical Research and Innovation Hospital was integrated into Kobe City Eye Hospital). The interpretation of the detected variants and the molecular diagnosis in each patient were discussed by a multidisciplinary team, including ophthalmologists, clinical geneticists, optometrists, nurses, researchers, and genetic counselors,[21] referring to the criteria and guidelines recommended by the American College of Medical Genetics and Genomics and the Association for Molecular Pathology.[24]

Statistical Analyses

The normality of the data distribution was tested using the Kolmogorov–Smirnov test. Intergroup analyses were performed using the unpaired *t*-test for continuous variables and the chi-square test for categorical variables. Correlations between the FAF abnormality area and the overall VFD area or between the EZ width and the central VF area were assessed using Spearman rank correlation coefficient. All statistical analyses were performed using the SPSS software package (version 28; SPSS Inc, Chicago, IL). The statistical significance of all tests was set at $P \leq 0.05$.

Results

This study included 16 eyes from 16 patients with BCD and 16 eyes from 16 patients with *RHO*-RP. The demographic and clinical characteristics of the patients are presented in Table 1.

Among the 16 patients with BCD, the mean age at examination was 61.0 ± 10.8 years and 13 patients were female. The median values of the FAF abnormality and overall VFD area were 98.5% (range, 13.6–100) and 57.5% (range, 9.8–98.5), respectively. The FAF abnormality areas covered posterior pole beyond vascular arcade in all 16 patients. The median value of the central VF area (within 30° in diameter) was 26.3% (range, 0–91.4). We observed visible EZ lines in 13 patients among 15 patients included in the OCT analyses, and the median EZ width on the cross-sections of central 30° was 504.3 μm (range, 0–5,305). The median LogMAR best-corrected visual acuity was 0.30 (range, −0.18 to 2.00). The correlation analyses indicated that the FAF abnormality area was not correlated with the overall VFD area. By contrast, there was significant correlation between the EZ width and the central VF area (r = 0.806, $P < 0.001$) (Figure 3). Only one patient with BCD (C1) with good image quality was examined at multiple visits over 3 years. At the first visit, RPE degeneration was observed throughout the fundus (FAF abnormality area was 100%). The overall VFD area increased from 94.0% at the first visit to 97.2% at 1 year, 97.5% at 2 years, 97.5% at 3 years, and 97.5% at 4 years after the first visit (Figure 4).

We analyzed 16 patients with *RHO*-RP for comparison. The mean age at examination was 53.9 ± 13.9 years, and 11 patients were female. No significant

Table 1. Demographic and Clinical Characteristics of the Study Participants

Index	Age at Examination (Years)	Sex	Eye	Gene	DNA Change	Protein Change	Age of Onset (Years)	Lens Status	BCVA	FAF Abnormality Area (%)	Overall VFD Area (%)	Central VF Area (Within 30° in Diameter) (%)	EZ Width on Central Cross-Sections (μm)	Macular Pathology
C1	63	F	R	CYP4V2	c.327+1G>A/c.802-8_810del17insGC	p.?/exon7del	16	IOL	0.3	100.0	94.0	26.8	303.8	
C2	68	F	L	CYP4V2	c.802-8_810del17insGC homo	exon7del	43	Clear	0.4	98.6	90.4	23.2	504	
C3	60	F	R	CYP4V2	c.518T>G/c.802-8_810del17insGC	p.L173W/exon7del	50	IOL	0.5	78.6	65.5	8.2	230.5	
C4	63	F	L	CYP4V2	c.518T>G/c.802-8_810del17insGC	p.L173W/exon7del	58	Clear	1.5	13.6	10.1	92.1	5,305	
C5	46	M	L	CYP4V2	c.327+1G>A/c.802-8_810del17insGC	p.?/exon7del	34	Clear	0.04	71.6	39.0	0	NA	Subretinal exudates
C6	81	M	L	CYP4V2	c.518T>G/c.802-8_810del17insGC	p.L173W/exon7del	47	Cataract	0.3	83.0	28.7	4.9	0	
C7	44	F	L	CYP4V2	c.518T>G/c.802-8_810del17insGC	p.L173W/exon7del	34	Clear	0.5	80.0	9.8	29.7	906.5	
C8	65	F	R	CYP4V2	c.802-8_810del17insGC homo	exon7del	46	Cataract	0.01	96.3	98.5	2.2	0	
C9	60	F	R	CYP4V2	c.802-8_810del17insGC homo	exon7del	39	Cataract	0.4	100.0	53.6	46.2	547.3	
C10	61	F	L	CYP4V2	c.802-8_810del17insGC homo	exon7del	40	Cataract	0.7	100.0	52.7	34.3	291	
C11	56	F	R	CYP4V2	c.802-8_810del17insGC homo	exon7del	42	Cataract	0.8	100.0	32.7	25.7	505.5	
C12	44	F	R	CYP4V2	c.802-8_810del17insGC homo	exon7del	33	Clear	1.2	98.3	19.4	28.5	643.3	
C13	78	F	L	CYP4V2	c.1020G>A homo	p.W340X	50	IOL	0.8	100.0	85.3	17.2	504.3	
C14	59	F	R	CYP4V2	c.802-8_810del17insGC homo	exon7del	36	Cataract	0.4	97.9	61.3	37.1	581.8	
C15	72	M	R	CYP4V2	c.518T>G/c.802-8_810del17insGC	p.L173W/exon7del	45	IOL	0.7	100.0	76.9	62.6	546.5	
C16	56	F	L	CYP4V2	c.802-8_810del17insGC/c.958C>T	exon7del/p.R320*	16	Cataract	0.7	100.0	61.8	7.4	0	
R1	51	F	R	RHO	c.173C>G	p.T58R	No symptoms	Clear	1.2	18.8	9.4	84.5	5,445	
R2	29	M	R	RHO	c.541G>A	p.E181K	10	Clear	1.2	96.2	78.4	64.2	1927	
R3	68	F	L	RHO	c.1005delT	p.T336fs	Early childhood	IOL	0.5	98.2	99.0	22.7	270.3	
R4	44	M	R	RHO	c.50C>T	p.T17M	Early childhood	Clear	1.2	23.1	16.4	82.1	5,148	
R5	90	F	R	RHO	c.1040C>T	p.P347L	5	IOL	0.03	100.0	99.3	16.9	174.8	
R6	63	F	R	RHO	c.1040C>T	p.P347L	Early childhood	IOL	0.9	100.0	97.7	51.7	NA	Epiretinal membrane
R7	67	F	R	RHO	c.1033G>A	p.V345M	10	Cataract	0.5	98.6	98.0	44.0	527.8	
R8	71	F	R	RHO	c.541G>A	p.E181K	44	Cataract	0.1	99.0	92.3	33.6	301.5	
R9	40	F	R	RHO	c.50C>T	p.T17M	No symptoms	Clear	1.2	8.2	15.9	90.5	3,998	
R10	39	F	R	RHO	c.568G>T	p.D190Y	15	Cataract	0.9	93.7	68.1	94.7	1,154	
R11	34	M	L	RHO	c.50C>T	p.T17M	No symptoms	Clear	1.5	25.0	23.0	99.1	6,800	
R12	55	F	L	RHO	c.810C>A	p.S270R	51	Cataract	0.8	27.6	33.9	48.6	1,210	
R13	42	M	L	RHO	c.403C>T	p.R135W	5	Clear	0.8	98.5	99.5	10.7	158.3	
R14	55	M	L	RHO	c.1040C>T	p.P347L	6	IOL	0.1	100.0	98.7	29.5	0	
R15	57	F	L	RHO	c.403C>T	p.R135W	Early childhood	IOL	0.04	99.1	99.9	1.5	NA	Epiretinal membrane
R16	60	F	L	RHO	c.1040C>T	p.P347L	13	IOL	LP	100.0	99.7	6.1	0	

BCVA, best-corrected visual acuity; IOL, intraocular lens; NA, not available.

Bietti crystalline dystrophy

A

B

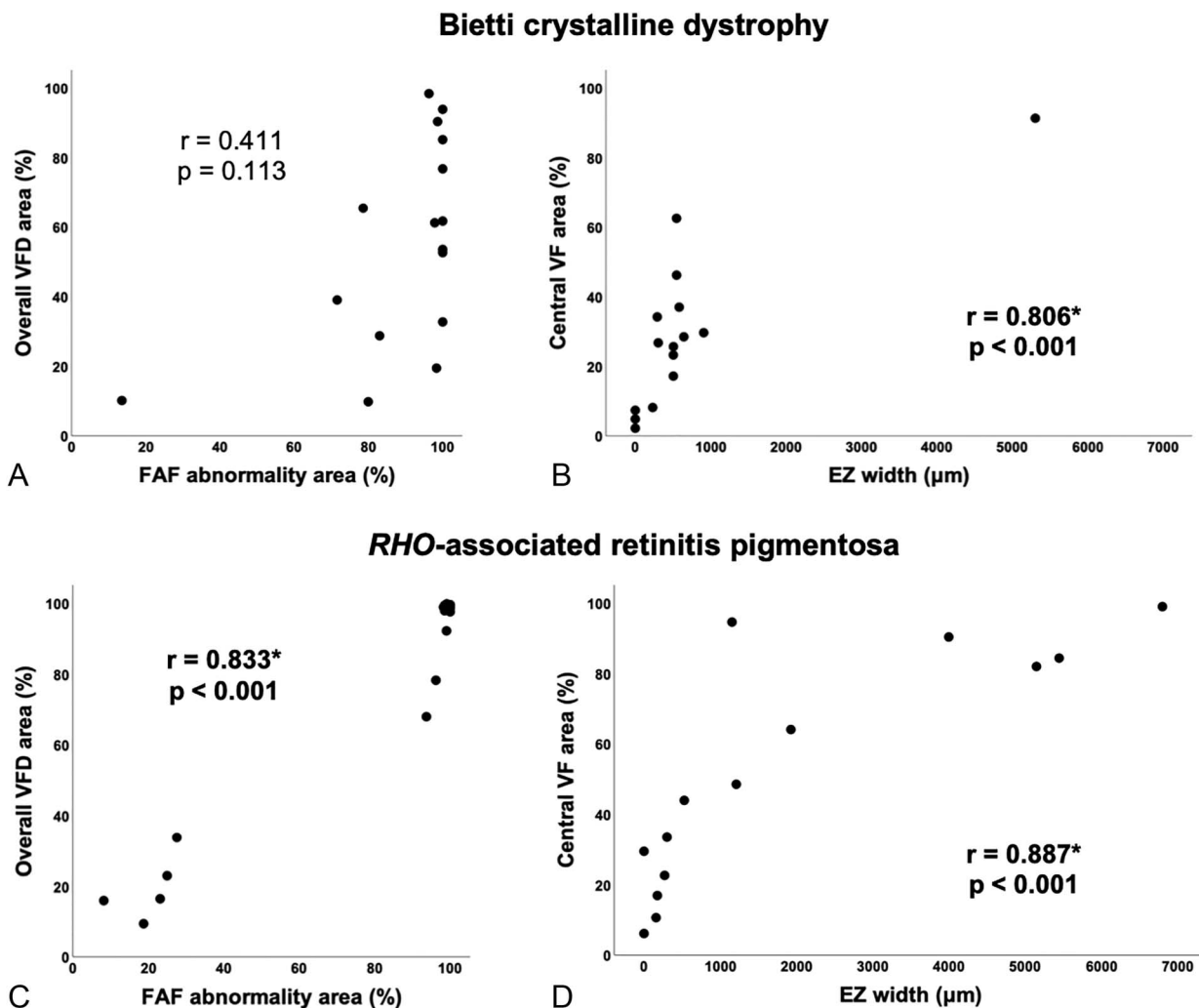## *RHO*-associated retinitis pigmentosa

C

D

Fig. 3. Scatterplots demonstrating the relationships between the FAF abnormality area and the overall VFD area (**A** and **C**) and those between the EZ width and the central VF area (**B** and **D**) in patients with BCD (upper panel) and *RHO-RP* (lower panel).

difference was observed in the mean age at examination and sex distribution between patients with BCD and *RHO*-RP. The median values of the FAF abnormality and overall VFD areas were 98.4% (range, 8.2–100) and 95.0% (range, 9.4–100), respectively. The median central VF area was 46.3% (range, 1.5–99.1), and the median LogMAR best-corrected visual acuity was 0.10 (range, −0.18 to 1.52). The median EZ width among 14 patients included in the OCT analyses was 840.9 μm (range, 0–6,800). In patients with *RHO*-RP, the FAF abnormality area was significantly correlated with the overall VFD area (r = 0.833, $P < 0.001$). Significant correlation between the central EZ width and the central VF area was also observed (r = 0.887, $P < 0.001$) (Figure 3). Correlations between the FAF abnormality area and the overall VFD area as well as between the central EZ width

and the central VF area in patients with BCD and *RHO*-RP are summarized in Table 2.

Discussion

This study investigated the relationship between the extent of RPE degeneration and that of photoreceptor damage or VF defects in two subtypes of IRDs: BCD and *RHO*-RP. We measured the FAF abnormality area and EZ width on OCT to evaluate the extent of RPE degeneration and that of photoreceptor damage, respectively. In patients with *RHO*-RP, we confirmed that both the FAF abnormality area and central EZ width had strong correlation with the VF measurements within relevant regions, which was consistent with previous reports.[11,14,25] The FAF abnormality observed in *RHO*-RP indicates RPE degeneration
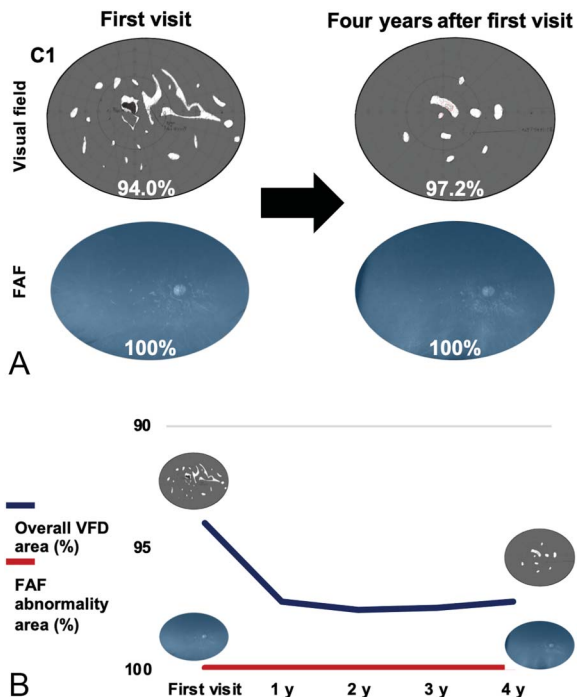
Fig. 4. Longitudinal observation of overall VFD and FAF abnormality areas over 4 years in a patient with BCD.

accompanied by photoreceptor damage. By contrast, in patients with BCD, the FAF abnormality area was not correlated with the overall VFD area and the overall VFD area was generally smaller than the FAF abnormality area. These findings demonstrate that the remaining VF exists within the FAF abnormality area, although the units of these two parameters, calculated by different methods, are not technically interchangeable. We can expect preservation of functional photoreceptor cells within the remaining VF with BCD, which is supported by the strong correlation between the central EZ width and the central VF area in the same patient group. Moreover, longitudinal data from a patient with BCD indicated that the VF defects had progressed within the preexisting FAF abnormality area, suggesting that the FAF abnormality in BCD reflects the preceding RPE degeneration, which is subsequently followed by photoreceptor degeneration and

vision loss. This interpretation seems compatible with the proposed disease mechanism of BCD, in which the RPE is primarily affected by lipid metabolism disturbance, followed by the secondary loss of overlying photoreceptors and visual function defects.[6,26,27]

Recent advancements in emerging therapies for IRDs have encouraged better characterization and categorization of genetically and clinically heterogeneous IRDs to assign appropriate therapy to patients. Pluripotent stem cell–derived RPE transplantation can be applied to the subgroup of IRDs with the primary pathology in RPE, including BCD, choroideremia,[28] and RP with a mutation in retinoid cycle-related genes, such as *RPE65*,[29] *LRAT*,[30] and *BEST1*,[31] or phagocytosis genes, such as *MERTK*.[32] We expect that these "RPE-impaired diseases"[33] can benefit from RPE transplantation to prevent secondary photoreceptor loss caused by the absence of the underlying RPE. We have detected discrepancy between RPE degeneration and VF defect in BCD as a characteristic retinal pathology, by analyzing the wide-field FAF and Goldmann perimetry, both of which enable evaluation of the whole retina. The preserved photoreceptors located on the degenerated RPE in such pathology would be a promising target for the RPE replacement therapy, including pluripotent stem cell–derived RPE transplantation. This study was not designed to assess heterogeneous findings that correspond to varying stages of disease progression in more advanced or less advanced regions within individual patients. Further research is necessary to ascertain the optimal therapeutic target regions and disease stage up to which patients may derive therapeutic benefit. The correspondence among the status of RPE, photoreceptors, and visual function at the same retinal regions is an important subject of interest. Polarization-sensitive OCT[34] and fundus-controlled perimetry (microperimetry)[35] could serve as modalities for evaluating focal status of RPE/photoreceptors and visual function, respectively.

In this study, we cut into the heterogeneity of RP by assessing only the patients with a single causative gene of *RHO*. We confirmed that the extent of FAF

Table 2. Correlations Between FAF Abnormality and Overall VFD Areas and Between EZ Width and Central VF Area in Patients With BCD and *RHO-RP*

	FAF Abnormality Area and Overall VFD Area		EZ Width and Central VF Area	
	r	Correlation	r	Correlation
BCD	0.411	None	**0.806***	Strong
RHO-RP	**0.833***	Strong	**0.887***	Strong

*Significant at $P < 0.05$ (bold font).
BCD, Bietti crystalline dystrophy.

abnormality and VF defects correlated well in patients with *RHO*-RP, which suggests that RPE degenerates shortly after or almost simultaneously as overlying functional photoreceptor loss. Although this correlation has been documented in patients with RP irrespective of the genotype,[11,14] the relationship between the RPE degeneration and visual function may differ according to the causative genes or underlying disease mechanisms. We consider that genotype-by-genotype assessment provides important insights that help organize the differences in disease mechanisms of IRDs.

The limitations of this study include the small sample size and cross-sectional design. Based on the findings obtained from the patient with longitudinal data, we suppose that the RPE degeneration precedes the VF defect in BCD; however, the manner of disease progression should be confirmed by future longitudinal studies involving larger samples.

In conclusion, FAF abnormality in patients with BCD involves the findings of RPE degeneration without complete loss of photoreceptors and visual function. Patients with BCD appear to be good candidates for the RPE replacement therapy for preservation of residual visual function on the degenerated RPE.

Key words: Bietti crystalline dystrophy, retina, retinal dystrophy, fundus autofluorescence, retinal pigment epithelium, retinal pigment epithelium transplantation, retinitis pigmentosa.

Acknowledgments

References

1. Wright AF, Chakarova CF, Abd El-Aziz MM, Bhattacharya SS. Photoreceptor degeneration: genetic and mechanistic dissection of a complex trait. Nat Rev Genet 2010;11:273–284.
2. Maeda T, Mandai M, Sugita S, et al. Strategies of pluripotent stem cell-based therapy for retinal degeneration: update and challenges. Trends Mol Med 2022;28:388–404.
3. Mandai M, Watanabe A, Kurimoto Y, et al. Autologous induced stem-cell–derived retinal cells for macular degeneration. N Engl J Med 2017;376:1038–1046.
4. Sugita S, Mandai M, Hirami Y, et al. HLA-matched allogeneic iPS cells-derived RPE transplantation for macular degeneration. J Clin Med 2020;9:2217.
5. Li A, Jiao X, Munier FL, et al. Bietti crystalline corneoretinal dystrophy is caused by mutations in the novel gene CYP4V2. Am J Hum Genet 2004;74:817–826.
6. Halford S, Liew G, Mackay DS, et al. Detailed phenotypic and genotypic characterization of Bietti crystalline dystrophy. Ophthalmology 2014;121:1174–1184.
7. Hata M, Ikeda HO, Iwai S, et al. Reduction of lipid accumulation rescues Bietti's crystalline dystrophy phenotypes. Proc Natl Acad Sci U S A 2018;115:3936–3941.
8. Yuzawa M, Mae Y, Matsui M. Bietti's crystalline retinopathy. Ophthalmic Paediatr Genet 1986;7:9–20.
9. Li Q, Li Y, Zhang X, et al. Utilization of fundus autofluorescence, spectral domain optical coherence tomography, and enhanced depth imaging in the characterization of Bietti crystalline dystrophy in different stages. Retina 2015;35:2074–2084.
10. Murakami Y, Koyanagi Y, Fukushima M, et al. Genotype and long-term clinical course of Bietti crystalline dystrophy in Korean and Japanese patients. Ophthalmol Retina 2021;5:1269–1279.
11. Oishi A, Ogino K, Makiyama Y, et al. Wide-field fundus autofluorescence imaging of retinitis pigmentosa. Ophthalmology 2013;120:1827–1834.
12. Delori FC, Dorey CK, Staurenghi G, et al. In vivo fluorescence of the ocular fundus exhibits retinal pigment epithelium lipofuscin characteristics. Invest Ophthalmol Vis Sci 1995;36:718–729.
13. Strauss O. The retinal pigment epithelium in visual function. Physiol Rev 2005;85:845–881.
14. Ogura S, Yasukawa T, Kato A, et al. Wide-field fundus autofluorescence imaging to evaluate retinal function in patients with retinitis pigmentosa. Am J Ophthalmol 2014;158:1093–1098.
15. Rossi S, Testa F, Li A, et al. An atypical form of Bietti crystalline dystrophy. Ophthalmic Genet 2011;32:118–121.
16. Athanasiou D, Aguila M, Bellingham J, et al. The molecular and cellular basis of rhodopsin retinitis pigmentosa reveals potential strategies for therapy. Prog Retin Eye Res 2018;62:1–23.
17. Koyanagi Y, Ueno S, Ito Y, et al. Relationship between macular curvature and common causative genes of retinitis pigmentosa in Japanese patients. Invest Ophthalmol Vis Sci 2020;61:6.
18. Lange C, Feltgen N, Junker B, et al. Resolving the clinical acuity categories "hand motion" and "counting fingers" using the Freiburg Visual Acuity Test (FrACT). Graefes Arch Clin Exp Ophthalmol 2009;247:137–142.
19. Holladay JT. Visual acuity measurements. J Cataract Refract Surg 2004;30:287–290.
20. Arai Y, Maeda A, Hirami Y, et al. Retinitis pigmentosa with EYS mutations is the most prevalent inherited retinal dystrophy in Japanese populations. J Ophthalmol 2015;2015:819760.
21. Maeda A, Yoshida A, Kawai K, et al. Development of a molecular diagnostic test for retinitis pigmentosa in the Japanese population. Jpn J Ophthalmol 2018;62:451–457.
22. Inaba A, Maeda A, Yoshida A, et al. Truncating variants contribute to hearing loss and severe retinopathy in USH2A-associated retinitis pigmentosa in Japanese patients. Int J Mol Sci 2020;21:7817.
23. Sakai D, Hiraoka M, Matsuzaki M, et al. Genotype and phenotype characteristics of RHO-associated retinitis pigmentosa in the Japanese population. Jpn J Ophthalmol 2023;67:138–148.
24. Richards S, Aziz N, Bale S, et al. Standards and guidelines for the interpretation of sequence variants: a joint consensus recommendation of the American College of Medical Genetics and Genomics and the Association for Molecular Pathology. Genet Med 2015;17:405–424.

25. Iriyama A, Yanagi Y. Fundus autofluorescence and retinal structure as determined by spectral domain optical coherence tomography, and retinal function in retinitis pigmentosa. Graefes Arch Clin Exp Ophthalmol 2012;250:333–339.

26. Rossi S, Testa F, Li A, et al. Clinical and genetic features in Italian Bietti crystalline dystrophy patients. Br J Ophthalmol 2013;97:174–179.

27. Lee KYC, Koh AHC, Aung T, et al. Characterization of Bietti crystalline dystrophy patients with CYP4V2 mutations. Invest Ophthalmol Vis Sci 2005;46:3812–3816.

28. Kalatzis V, Hamel CP, MacDonald IM, First International Choroideremia Research Symposium. Choroideremia: towards a therapy. Am J Ophthalmol 2013;156:433–437.e3.

29. Kiser PD. Retinal pigment epithelium 65 kDa protein (RPE65): an update. Prog Retin Eye Res 2022;88:101013.

30. Talib M, van Schooneveld MJ, van Duuren RJG, et al. Long-term follow-up of retinal degenerations associated with LRAT mutations and their comparability to phenotypes associated with RPE65 mutations. Transl Vis Sci Technol 2019;8:24.

31. Johnson AA, Guziewicz KE, Lee CJ, et al. Bestrophin 1 and retinal disease. Prog Retin Eye Res 2017;58:45–69.

32. Feng W, Yasumura D, Matthes MT, et al. Mertk triggers uptake of photoreceptor outer segments during phagocytosis by cultured retinal pigment epithelial cells. J Biol Chem 2002;277:17016–17022.

33. Maeda T, Sugita S, Kurimoto Y, Takahashi M. Trends of stem cell therapies in age-related macular degeneration. J Clin Med 2021;10:1785.

34. Pircher M, Hitzenberger CK, Schmidt-Erfurth U. Polarization sensitive optical coherence tomography in the human eye. Prog Retin Eye Res 2011;30:431–451.

35. Pfau M, Jolly JK, Wu Z, et al. Fundus-controlled perimetry (microperimetry): application as outcome measure in clinical trials. Prog Retin Eye Res 2021;82:100907.